Published in final edited form as:
Cell Tissue Res. 2009 September ; 337(3): 407–428. doi:10.1007/s00441-009-0826-6.

Defects in the cerebella of conditional *Neurod1* null mice correlate with effective *Tg(Atoh1-cre)* recombination and granule cell requirements for *Neurod1* for differentiation

Ning Pan,
Department of Biology, College of Liberal Arts and Sciences, University of Iowa, 143 BB, Iowa City, IA 52242, USA; Department of Molecular, Cellular and Developmental Biology, University of Colorado, Boulder, CO 80309, USA

Israt Jahan,
Department of Biology, College of Liberal Arts and Sciences, University of Iowa, 143 BB, Iowa City, IA 52242, USA

Jacqueline E. Lee, and
Department of Molecular, Cellular and Developmental Biology, University of Colorado, Boulder, CO 80309, USA

Bernd Fritzsch
Department of Biology, College of Liberal Arts and Sciences, University of Iowa, 143 BB, Iowa City, IA 52242, USA

Abstract

Neurod1 is a crucial basic helix-loop-helix gene for most cerebellar granule cells and mediates the differentiation of these cells downstream of *Atoh1*-mediated proliferation of the precursors. In *Neurod1* null mice, granule cells die throughout the posterior two thirds of the cerebellar cortex during development. However, *Neurod1* is also necessary for pancreatic β-cell development, and therefore *Neurod1* null mice are diabetic, which potentially influences cerebellar defects. Here, we report a new *Neurod1* conditional knock-out mouse model created by using a *Tg(Atoh1-cre)* line to eliminate *Neurod1* in the cerebellar granule cell precursors. Our data confirm and extend previous work on systemic *Neurod1* null mice and show that, in the central lobules, granule cells can be eradicated in the absence of *Neurod1*. Granule cells in the anterior lobules are partially viable and depend on as yet unknown genes, but the Purkinje cells show defects not previously recognized. Interestingly, delayed and incomplete *Tg(Atoh1-cre)* upregulation occurs in the most posterior lobules; this leads to near normal expression of *Neurod1* with a concomitant normal differentiation of granule cells, Purkinje cells, and unipolar brush cells in lobules IX and X. Our analysis suggests that *Neurod1* negatively regulates *Atoh1* to ensure a rapid transition from proliferative precursors to differentiating neurons. Our data have implications for research on medulloblastoma, one of the most frequent brain tumors of children, as the results suggest that targeted overexpression of *Neurod1* under *Atoh1* promoter control may initiate the differentiation of these tumors.

bernd-fritzsch@uiowa.edu .

Present Address: J. E. Lee, Geron Corporation, 230 Constitution Drive, Menlo Park, CA 94025, USA

Ning Pan and Israt Jahan contributed equally to this paper.

Keywords

Granule cell development; Cerebellum; Proliferation regulation; Cell death; bHLH genes; Mouse (*Neurod1* null)

Introduction

The production of neurons requires the complex integration of extra- and intracellular factors to control the balance between proliferation, differentiation, migration, and survival. Since the cerebellum was first used by Ramón y Cajal to establish the neuron theory (Sotelo 2008), this regular cytology has provided insights into neuroanatomical and physiological problems. In recent decades, the cerebellum has evolved into a system for studying central nervous system (CNS) development at the molecular level, by combining morphogenetic movements, neuronal cytological maturation, and the establishment of neuronal layers (Hatten and Heintz 1995; Sgaier et al. 2005). This increased interest has in part been triggered by the derailment of proliferation regulation in medulloblastoma cases (Leung et al. 2004; Barisone et al. 2008; Schuller et al. 2008). Despite the complexity of the cerebellum at the level of the molecular coding of development, the cerebellar cortex is histologically uniform and divided into three distinct cellular layers in the adult: the molecular layer (ML), the Purkinje cell layer (PCL), and the granule cell layer (GCL; Mugnaini et al. 1997). The most superficial ML contains stellate and basket cell interneurons, dendrites of Purkinje cells (PCs), axons of granule cells (GCs; parallel fiber), and Bergmann glia processes (Voogd and Glickstein 1998). The next layer (PCL) comprises the somata of PCs and also the somata of the Bergmann glia (Voogd and Glickstein 1998). The innermost GCL lying above the white matter consists of the most numerous neuronal cell type of the brain, GCs, in the majority of the layer and the somata of Golgi cell and unipolar brush cells (UBCs) predominantly in the posterior lobules (lobules IX and X; Mugnaini et al. 1997).

The formation of the cerebellum spans embryonic and postnatal development, initiating at embryonic day 9 (E9) in the mouse (Hatten and Heintz 1995; Larramendi 1969; Fujita et al. 1966; Fujita 1969). Two primary regions are thought to give rise to the neurons that make up the cerebellum. The first region is the ventricular zone in the roof of the fourth ventricle, this region produces γ-aminobutyric acid (GABA)ergic neurons, including PCs, Golgi, basket, stellate cells, and small deep cerebellar nuclei neurons (Hatten and Heintz 1995; Hoshino et al. 2005). Precursors of the cerebellar GCs are generated in the second germinal zone, which is called the rhombic lip (Englund et al. 2006; Machold and Fishell 2005; Wang et al. 2005). They proliferate and migrate anteromedially from the lateral caudal portion to the outer pial surface of the developing cerebellum between E13 and E16 to form the external granular layer (EGL; Alder et al. 1996; Altman and Bayer 1978; Hatten et al. 1982). The cells of the outer layer of the EGL continue to proliferate after birth, when the postmitotic cells in the inner EGL begin to differentiate and migrate radially into the cerebellar cortex along the processes of the Bergmann glia cells to form the internal granular layer (IGL; Fujita et al. 1966; Hatten et al. 1982). Cerebellar GCs form up to 60% of the total CNS neurons in mammals and derailment of proliferation leads to the most common brain tumor in children, forming up to 30% of pediatric tumor cases (Barisone et al. 2008). Understanding the regulation and differentiation in the cerebellum is thus of significant clinical and basic scientific importance. We focus here on the molecular basis of the differentiation pathway of cerebellar GCs on the premise that the initiation of differentiation might combat uncontrolled proliferation as found in medulloblastomas.

Proteins of the basic helix-loop-helix (bHLH) class play a central role in the determination of neuronal lineages in the peripheral nervous system (PNS) and CNS (Bertrand et al. 2002; Kageyama et al. 2007). The bHLH protein *Neurod1* is widely expressed in both CNS and PNS in vertebrates (Lee et al. 1995). Ectopic expression of *Neurod1* in *Xenopus* neural ectoderm leads to neuronal differentiation, suggesting that *Neurod1* regulates the formation of neurons from neural precursors (Lee et al. 1995). In the mouse CNS, a high level of *Neurod1* expression is found in differentiating neurons and in mature neurons such as the GCs of the cerebellum, inferior colliculus, and hippocampus, and the neurons of the limbic system (Lee 1997; Gurung and Fritzsch 2004). In the PNS, *Neurod1* expression is found in developing and mature sensory neurons (Lee et al. 1995; Kim et al. 2001). For example, during inner ear development, *Neurod1* expression is first detected in the sensory neuroblast precursors as early as E8.75 (Ma et al. 1998). Consistently, *Neurod1* null mutants have severe reduction of vestibular neurons and near complete loss of cochlear neurons in the ear (Kim et al. 2001).

Neurod1 expression in the cerebellum correlates with the differentiation of GCs (Dahmane and Ruiz-i-Altaba 1999; Goldowitz and Hamre 1998). *Neurod1* is highly expressed in both EGL and IGL of the cerebellum between postnatal day 5 (P5) and P13, and the IGL expression persists at a stable level until adulthood (Lee et al. 2000; Miyata et al. 1999). Despite the near uniform histology throughout its lobules, the cerebellum has divergent expression pattern of certain genes in various lobules of the cerebellum. For example, the anterior lobules of the cerebellum are able to undergo some near normal development without *Neurod1* (Miyata et al. 1999; Cho and Tsai 2006). In contrast, an absence of *Neurod1* leads to a near total loss of GCs and disarrangement of PCs in the posterior lobules (Miyata et al. 1999;Cho and Tsai 2006). *Atoh1*, another bHLH gene, is expressed in cerebellar GC precursors (GCPs) at the rhombic lip and in the outer EGL in the developing cerebellum (Akazawa et al. 1995; Ben-Arie et al. 1996, 1997; Helms et al. 2000). Genomic disruption has established that *Atoh1* is essential for the proper development of cerebellar GCs, as *Atoh1* null mice lack the EGL (Ben-Arie et al. 1997; Helms et al. 2000) and other *Atoh1*-dependent brain areas (Wang et al. 2005; Fritzsch et al. 2006a). However, overexpression of *Atoh1* disrupts neural differentiation in normal cerebellar development (Gazit et al. 2004; Helms et al. 2001; Isaka et al. 1999), implying an interaction (not as yet fully characterized) with *Neurod1* in the regulation of proliferation and differentiation.

In the present study, we have used a *Tg(Atoh1-cre)* (Matei et al. 2005) to eliminate a loxP-flanked *Neurod1* (Goebbels et al. 2005) in the developing cerebellum to sidestep the diabetic condition in *Neurod1* null mice, thus avoiding the additional systemic effects of low or limited insulin production known to cause various neuropathies. Previous work has demonstrated that delayed elimination of floxed *Neurod1* in mature cerebellar GCs does not cause any defects despite the continued expression of *Neurod1* in those GCs (Goebbels et al. 2005). In contrast to this absence of any recognizable defects in near adult *Neurod1* conditional null mice, we have found a gradient of *Neurod1* loss and concomitant defects in cerebellar development in our conditional model that eliminates *Neurod1* prior to cerebellar GC differentiation in most lobules. However, the posterior lobules (1/2VIII + IX + X) do not lose all of the *Neurod1* expression and show near normal morphology. In agreement with the more recent insights into the complexity of transcription initiation (Buratowski 2008), we suspect that insufficient and delayed upregulation of *Tg(Atoh1-cre)* in the posterior lobules is incompatible with the excision of the floxed *Neurod1*. The central lobules (VI + VII + 1/2VIII) show complete absence of *Neurod1* and massive loss of all GCs. In situ hybridization analysis indicates that *Atoh1* acts in these lobules in a negative feedback loop with *Neurod1*. *Atoh1* expands its expression in continuously proliferating precursor populations in the absence of *Neurod1*. These GCs eventually all die without ever migrating in a coordinated fashion into the IGL. We also find disorganization of PC distribution and

orientation in these cerebellar lobules of *Neurod1* conditional mutant mice. As expected based on previous work (Miyata et al. 1999; Cho and Tsai 2006), loss of *Neurod1* in the anterior lobules is partially rescued by an as yet unknown transcription factor that compensates the need for *Neurod1* in differentiating GCs. We confirm this previous finding and our more detailed analysis shows aberrations in the PC dendritic trees previously unrecognized in systemic *Neurod1* null mice in these lobules.

Materials and methods

Mice and genotyping

Generation of mice variously genotyped as *Neurod1* null (Miyata et al. 1999), floxed *Neurod1* (Goebbels et al. 2005), and *Tg(Atoh1-cre)* with a ROSA26 reporter (Matei et al. 2005) was as described previously. Conditional *Neurod1* null mice were generated by breeding homozygotic floxed *Neurod1* mice (*Neurod1*$^{f/f}$) with *Neurod1*$^{f/+}$,*Tg(Atoh1-cre)* mice. The resulting *Neurod1*$^{f/f}$,*Tg(Atoh1-cre)* mice were used as *Neurod1* conditional mutant, and the *Neurod1*$^{f/+}$,*Tg(Atoh1-cre)* heterozygous siblings were used as controls. Tail biopsies were used for genomic DNA preparation, and polymerase chain reaction analysis was performed for genotyping. Animal procedures were performed in accordance with IACUC guidelines for use of laboratory animals in biological research.

X-gal staining

Heads of mice perfused with 4% paraformaldehyde were hemisected, and cerebella were dissected and then briefly washed with phosphate buffer. The samples were stained in a solution containing 0.1 M phosphate buffer, 1% deoxycholic acid, 2% NP40, 1 mM magnesium chloride, 0.5 M potassium ferricyanide, 0.5 M potassium ferrocyanide, and 2 mg/ml X-gal (5-bromo-4-chloro-3-indolyl-β-D-galactoside) for 24 h at room temperature (Matei et al. 2006).

In situ hybridization

In situ hybridization was performed with the RNA probe labeled with digoxigenin. The plasmids containing the cDNAs were used to generate the RNA probe by in vitro transcription. The dissected cerebella were fixed in 0.4% paraformaldehyde and digested briefly with 10 μg/ml Proteinase K (Ambion, Austin, Tex., USA) for 15–20 min. The samples were then hybridized overnight at 60°C to the riboprobe in hybridization solution containing 50% formamide, 50% 2× saline sodium citrate, and 6% dextran sulfate. After the unbound probe had been washed off, the samples were incubated overnight with an anti-digoxigenin antibody (Roche Diagnostics, Mannheim, Germany) conjugated with alkaline phosphatase. After a series of washes, the samples were reacted with nitroblue phosphate/5-bromo, 4-chloro, 3-indolil phosphate (BM purple substrate, Roche Diagnostics, Germany), which is enzymatically converted to a purple-colored product. Reacted parts were mounted flat in glycerol and viewed in a Nikon Eclipse 800 microscope by using differential interference contrast microscopy. Images were captured with Image-Pro software.

Immunocytochemistry

For immunocytochemical staining, 100-μm sagittal sections of cerebellum were defatted in 70% ethanol overnight and blocked with 5% normal goat serum in PBS containing 0.1% Triton X-100 for 2 h. The primary antibodies for active caspase 3 (Cell Signaling Technology), calbindin (Sigma), and calretinin (Chemicon) were then used at dilutions of 1:100, 1:500, and 1:400, respectively and incubated on the sections for 48 h at 4°C. After several washes with PBS, corresponding secondary antibodies (1:500; conjugated to Alexa dyes) were added and incubated on the sections overnight at 4°C. The sections were washed

with PBS, counter-stained with Hoechst stain, and mounted in glycerol. Images were taken via a Leica TCS SP5 confocal microscope.

Lipophilic dye tracing

Lipophilic-dye-soaked filter strips (Fritzsch et al. 2005) were inserted into the cerebellar folia parasagittally to label parallel fibers. We also labeled PCs dendrites by shooting lipophilic dye bullets coated with tungsten particles into the 200-μm parasagittal cerebellar sections (Benediktsson et al. 2005).

Plastic embedding and Stevenel's blue staining

Thick parasagittal sections of cerebellum were fixed in 2.5% glutaraldehyde overnight followed by several washes with 0.1 M phosphate buffer and then fixed with 1% osmium tetroxide for 1 h. Samples were then dehydrated in graded ethanol and propylene oxide, embedded with Epon 812 in beam capsules, and baked at 60°C for 48 h. Sections (2 μm) were cut by using an Ultratome and stained with Stevenel's blue (del Cerro et al. 1980), composed of 2% potassium permanganate and 1.3% methylene blue, at 60°C.

Body weight and blood glucose measurement

Mice were weighed at the specified age, and tail vein blood was then used to determine the blood glucose concentration by the FreeStyle flash blood glucose monitoring system (Therasense).

Area measurement

We took three different sagittal sections of cerebellum of various ages to measure the area of total cerebellum and the area of lobule X and then calculated the percentage between them. We also measured the thickness of EGL in micrometers in three different areas and calculated the mean. We counted GC numbers in a 40-μm region along the thickness of the EGL and calculated the mean of three counts in three different areas. We used Image-Pro software to perform the calibrated measurements.

Results

Conditional *Neurod1* knock-out mice

Previous studies have shown that *Neurod1* can convert non-neuronal ectodermal cells into fully differentiated neurons. In addition, *Neurod1* is expressed abundantly in mature neurons in adult brain structures, including the hippocampus and cerebellum, which suggests a secondary role of *Neurod1* in fully differentiated neurons (Lee et al. 1995).

In this study, we analyzed the function of *Neurod1* in postnatal murine cerebellum by using *Neurod1* conditional knock-out mice [*Neurod1*$^{f/f}$*,Tg(Atoh1-cre),ROSA26*]. We employed an *Atoh1* promoter fragment to drive Cre recombinase. Cre-mediated excision of the floxed *Neurod1* gene results in deletion of *Neurod1* only in the region where *Tg(Atoh1-cre)* is expressed, which can be monitored by β-galactosidase staining resulting from the Cre-mediated activation of the ROSA26-lacZ reporter (Matei et al. 2005). *Neurod1* heterozygous littermates [*Neurod1*$^{f/+}$*,Tg(Atoh1-cre ROSA26*] were used as controls. In contrast to the systemic *Neurod1* null mice, which died within a few days after birth because of severe hyperglycemia, our *Neurod1* conditional knock-out mice survived to adulthood. We measured their body weight and blood glucose and found no abnormality when compared with control *Neurod1* heterozygous mice (Table 1). Therefore, we could successfully circumvent the effect of *Neurod1* in pancreatic β-cell development in our conditional mouse model.

Effect of delayed *Tg (Atoh1-cre)* upregulation in cerebellum

Previous work has shown that *Atoh1* is necessary for cerebellum formation (Wang et al. 2005; Bermingham et al. 2001). We first examined *Tg(Atoh1-cre)* expression in the cerebellum by analyzing the β-galactosidase distribution in both *Neurod1* conditional knock-out and control heterozygous mice aged P2, P11, P15, and P21 and in adults over one year of age. At P2, *Tg(Atoh1-cre)* showed expression from lobules I through VIII. This expression had progressed to lobule IX by P11, to one third of lobule of X by P15, and to half of lobule X by the adult stage (Fig. 1a-e). The onset of *Tg(Atoh1-cre)* upregulation was delayed in the posterior lobules (IX + X), and this insufficient *Tg(Atoh1-cre)* upregulation apparently led to the failure of excision of floxed *Neurod1* in these lobules, as demonstrated by in situ hybridization for *Neurod1* (Fig. 1f'-j'). Indeed, *Neurod1* expression remained unchanged at later stages, even after *Tg(Atoh1-cre)* started to be expressed in the posterior lobules, suggesting that *Tg(Atoh1-cre)* was effectively recombining at the embryonic expression levels, with the later increase shown by ROSA26-lacZ being ineffective.

We have previously shown that, in developing cochlear nucleus and spiral neurons, *Tg(Atoh1-cre)* is expressed only days after *Neurod1* is upregulated (Kim et al. 2001;Fritzsch et al. 2006a; Matei et al. 2005; Bulfone et al. 2000). Consistent with this, the floxed *Neurod1* could not be excised by delayed *Tg(Atoh1-cre)* upregulation, and we detected normal expression of *Neurod1* in these cochlear nuclei and neurons in mutant ears (Fig. 2).

Severe loss of GCs in central lobules

All GCs in the central lobules (1/2VI–1/2VIII) of the cerebellum were lost in adult *Neurod1* conditional mutant mice (Figs. 1, 3e, f). However, this loss was not attributable to the failure of GC to proliferate. At P11, the EGL was near normal in thickness, but GCs dispersed and migrated radically in these lobules from the EGL to the IGL. All GCs degenerated with progression of time (Fig. 3a-f), and the majority of GCs had disappeared by P21 (Fig. 3d). We further evaluated the degeneration of GCs through analysis of pyknotic nuclei by Hoechst stain, by Stevenel's stain in thin sections, and by activated caspase 3 immunocytochemistry. In the central lobules of mutant cerebellum, the degeneration of GCs was evident by the presence of many pyknotic nuclei in the EGL (Fig. 4b, d-d", Table 2, see also Changes of EGL over time). In addition, these pyknotic nuclear profiles co-localized with activated caspase 3 (Fig. 4d-d"), clearly demonstrating that GCs underwent apoptosis in the absence of *Neurod1*. Although the anterior lobules were organized more orderly, many pyknotic changes were observed with activated caspase-3-positive nuclei in GCs (Fig. 4a, Table 2, see also Changes of EGL over time), consistent with the reduction of GCs reported in systemic *Neurod1* null mice (Miyata et al. 1999).

The GC depletion in central lobules was also seen in $Neurod1^{f/Z}$, *Tg(Atoh1-cre)* mice, which carry a *Neurod1* null allele that contains the *lacZ* reporter gene in place of the *Neurod1* coding region at the *Neurod1* locus. The X-gal staining reflected the endogenous *Neurod1* expression pattern and showed a near total loss of GCs in the central lobules in the adult mutant cerebellum (Fig. 5b-b"). In *Neurod1* heterozygous mice, the cerebellum developed uniformly in all lobules (Fig. 5a, a'), indicating the lack of dosage effect of *Neurod1* on GC differentiation.

Presence of *Neurod1* rescued lobules IX and X in mutant cerebellum

In contrast to the severe loss of GCs in the central lobules, lobules IX and X in mutant cerebellum had near normal cytoarchitecture, and lobule X was the closest to wildtype size among all the lobules. Since the total area of the cerebellum was reduced to about half in the mutant, the relative area of lobule X was nearly doubled in mutant compared with the heterozygous control (Fig. 6). The GCs in the EGL and IGL were normally arranged in

lobules IX and X and in up to half of the lobule VIII in mutant mice; this was consistent with the residual expression of *Neurod1*, as shown by in situ hybridization in these lobules (Fig. 7a). Massive disorganization of GCs was observed from the point at which the *Neurod1* gene was deleted in the mutant (Fig. 7a, c). Moreover, no distinct demarcation was seen between the EGL, ML, PCL, and IGL in central lobules in the mutant (Fig. 7b), although in lobules IX and X, the organization of these layers was almost normal compared with that in control cerebellum (Fig. 7d). This demonstrates that the presence of *Neurod1* can save the development of one lobule in the same cerebellum in which the others are affected severely by the absence of *Neurod1*. This internal control allows us to correlate directly the histological differences in the various lobules with the conditional deletion of *Neurod1* and the requirement of GCs for *Neurod1* for their differentiation.

Neurod1 mutation influences survival of GCs but not UBCs

Consistent with the degree of activated caspase-3-positive GC nuclei in neonate (Fig. 4), we have seen reduced survival to massive loss of GCs in anterior to central lobules, respectively, in adult mutant cerebellum (Fig. 8d) analyzed by Hoechst stain. The density of GCs only in the posterior lobules of the mutant (Fig. 8d') were comparable with heterozygous mice (Fig. 8a, a'), whereas the loss of GCs in other lobules was only clearly noticeable.

We also analyzed the morphology of UBCs in *Neurod1* mutant cerebellum by immunocytochemistry with calretinin, a specific marker for UBCs. The distribution of UBCs was mainly restricted to lobules X and half of IX (Fig. 8b-c'), consistent with a previous report (Dino et al. 1999). The morphology and distribution of UBCs has not changed in the mutant cerebellum because of the retention of *Neurod1* in the posterior lobules, which rescued UBCs (Fig. 8e-f') together with GCs and PCs. The presence of a normal posterior lobule provided intrinsic controls for sagittal slice results, and thus, this mouse model allowed us directly to assess the postnatal functions of the GCs in the cerebellar cortex in the same preparation.

Changes of EGL over time

We next measured the thickness of the EGL and semi-quantified the number of GCs in the EGL of various ages and in various lobules (Table 2). In the heterozygous cerebellum, the thickness of the EGL was reduced linearly with age as development proceeded, and as GCs migrated to the IGL (Fig. 9a-a"'). However, in *Neurod1* conditional mutant mice, both the thickness of the EGL and the number of GCs in lobule VII were increased in P11 compared with P7 (Fig. 9c-c'), whereas in the posterior half of lobule VIII or in lobules IX or X (Fig. 9b-b"'), they were comparable with the heterozygous cerebellum (Table 2). At all ages, the EGL, ML, PCL, and IGL were distinctly developed and could be distinguished clearly in the heterozygous cerebellum (Fig. 9a-a"'). In the conditional *Neurod1* mutant cerebellum, all layers of the cerebellum were severely disrupted in the central lobules. In lobule VII of the mutant cerebellum, there was no ML, as all the GCs were scattered and dispersed in and out of the EGL (Fig. 9c-c"'). Pyknotic nuclei were most apparent in lobules VI-VIII (Fig. 9c-c") but also found in lobules I-V (Fig.9d-d'). In the posterior half of lobule VIII, in which *Neurod1* gene was retained, the layers were less disorganized than in the rest of the central lobules.

GCs depletion is directly proportional to organization of PCs and their dendritic arborization

PCs are an integral component of the cytoarchitecture of the cerebellar cortex, with their orderly alignment in the monolayer and their planar dendritic arbor. In the mouse, PCs cease to divide at about E12 and form a monolayer at about postnatal day 10 (Miale and Sidman

1961). Dendritic trees of PCs develop dramatically during the second and third postnatal weeks (Larramendi 1969; Weiss and Pysh 1978; Mugnaini 1969), and this development appears to depend on the proper formation of parallel fibers, the axons of GCs (Bradley and Berry 1978).

To assess the morphology of PCs in the *Neurod1* conditional null mice, we performed immunocytochemistry with an antibody against calbindin in the adult cerebellum (Fig. 10). We found severely disorganized PCL in the anterior and central lobules (lobules I–VIII) of the cerebellum of *Neurod1* mutant mice (Fig. 10c-d", e', e"). In contrast, the PCs formed a monolayer with a normal orientation of their dendrites in lobules IX and X (Fig. 10b-b"), as in the heterozygous cerebellum (Fig. 10a-a", e). In central lobules (lobules VI-1/2VIII), PCs were dispersed randomly and showed no definite polarity of their dendrites (Fig. 10c-c", e'). Interestingly, although the organization of the GCL and the ML of the anterior lobules was nearly normal with only some GC loss, PCs formed a disorganized monolayer, with either weeping-willow-like dendrites or bidirectional dendrites projecting toward both the pia surface and the GCL (Fig. 10d-d", e").

Some disorganization of PCs found in lobules VI-VIII has previously been reported in the posterior region of the cerebellum in systemic *Neurod1* null mutants (Miyata et al. 1999; Cho and Tsai 2006) and has been suggested to be secondary to GC loss. By lipophilic dye tracing, we have, for the first time, demonstrated the abnormal orientation of PC dendrites in the cerebellum of *Neurod1* mutant mice (Fig. 10e', e") and shown that, in the anterior lobules, many PCs have bifurcated dendrites (Fig. 10e").

Loss of GCs affects distribution of mossy fibers

Cerebellar GCs are innervated by mossy fibers and thus relate mossy fiber input to PCs. Agranular cerebella have previously been generated by other means (Berry and Bradley 1976; Sotelo 1975; Arsenio Nunes et al. 1988), but the effect of the absence of GCs on the mossy fiber input into the cerebellum has not been systematically investigated with modern tracing techniques. The differential effects of our conditional deletion of *Neurod1* in various lobules allow us directly to compare the innervations of mossy fibers in the neighboring lobules by using lipophilic dye tracing.

Parasagittal insertions of lipophilic dye-soaked filter strips resulted in the labeling of parallel fibers along a given folium (Fig. 11) for a variable distance parallel to the insertion site. However, in mutant cerebellum, parallel fibers could not be traced in lobule VI through the anterior part of lobule VIII, thus confirming the complete absence of parallel fibers because of the complete absence of GCs in these lobules. Interestingly, instead of having parallel fibers extending medio-lateral, these lobules showed mossy fibers extending laterally beyond the point at which they could be traced in lobules IX and X. This implies that, in the absence of GCs, the parasagittal organization of mossy fibers is in part disrupted. The extent to which they are disrupted requires additional analysis through direct tracing of these inputs from their sources with lipophilic dyes.

The organization of mossy fibers was not only disrupted in a medio-lateral plane but also within a given folium. Whereas only climbing fibers could be traced into the ML in wildtype cerebella and folia IX + X in the conditional *Neurod1* mutants, we found many fibers running, some even partially myelinated, throughout the folium and underneath the pia surface (Fig. 11b). These data imply that the contact between mossy fibers and GCs is needed to stop extension of those fibers into the ML and to restrict them to this layer. As previously indicated in agranular cerebella (Sotelo 1975;Arsenio Nunes et al. 1988), mossy fibers might be able to contact PC dendrites directly in the absence of GCs. We are currently

investigating this possibility with appropriate double- and triple-color tracing with lipophilic dyes (Jensen-Smith et al. 2007).

In summary, GCs may not only be relevant for the normal formation of cerebellar layers, the alignment of PCs, and the proper development of PC dendrites, but may also play a role in the organization of the cerebellar mossy and climbing fiber input. In the absence of GCs, mossy fibers might behave like climbing fibers, an idea that we are currently testing in a longitudinal study of mossy and climbing fiber development in postnatal conditional *Neurod1* null mice.

Atoh1 expression in *Neurod1*-depleted area

Neural bHLH transcription factors have specific roles in cerebellar development, and their expression needs to be precisely controlled both spatially and temporally as neuronal precursors mature. *Atoh1* is a bHLH transcriptional factor homologous to the proneural factor *atonal* in *Drosophila. Atoh1* is one of the earliest markers of cerebellar GC progenitors, and its expression is turned off as the GCs in EGL exit the cell cycle and begin to differentiate and migrate inward to become mature GCs in the IGL (Alder et al. 1999).

In our *Neurod1* heterozygous mice, *Atoh1* was expressed in the outer EGL with a gradient that was higher in the anterior lobules than in the posterior lobules at P7 and P11 (Fig. 12a–b'). At P15, *Atoh1* expression was abolished in almost all lobules, except for some retention in lobule VII (Fig. 12c, c'), the last lobule to differentiate (Joyner and Zervas 2006). No *Atoh1* expression was detectable by in situ hybridization at P21 or older (data not shown). However, in our *Neurod1* mutant mice, *Atoh1* expression remained turned on for longer and was expanded compared with the control cerebellum. At P7, *Atoh1* was expressed in a similar pattern in mutant cerebellum as in heterozygous cerebellum (Fig. 12a, d). However, in the central lobules in P11 mutants, *Atoh1* was abnormally expanded inwardly toward the ill-defined inner EGL and IGL (Fig. 12e, e'). *Atoh1* expression was also discernable in the P15 mutant, with a gradient that was higher in the anterior and central lobules and almost absent in lobules IX and X, the lobules in which *Neurod1* expression was preserved because of delayed upregulation of *Tg(Atoh1-cre)* (Fig. 12f, f').

Barhl1 expression in *Neurod1* mutant cerebellum

The transcription factor *Barhl1* is one of the few known downstream genes of *Atoh1* and is expressed in the developing inner ear hair cells, cerebellar GCs, precerebellar neurons, and collicular neurons (Bulfone et al. 2000; Chellappa et al. 2008; Higashijima et al. 1992; Kojima et al. 1991; Li et al. 2002). *Barhl1* plays a crucial role in the migration and survival of cerebellar GCs and certain precerebellar neurons by governing the expression of *Neurotrophin3* (*Ntf3*; Li et al. 2004). Li et al. (2004) have shown that the absence of *Barhl1* causes increased GC death and concomitant loss of mossy-fiber-forming precerebellar neurons. Therefore, we have analyzed the expression of *Barhl1* in the *Neurod1* mutant cerebellum.

In the *Neurod1* heterozygous cerebellum, *Barhl1* was homogeneously expressed in all lobules in the EGL, whereas in the IGL, a gradient was present showing more prominent expression in lobules I-VI and lower expression in lobules IX and X (Fig. 13a-c). In *Neurod1* conditional mutant cerebellum, *Barhl1* was expressed prominently in the EGL, but the expression in IGL was almost abolished from P11 onward (Fig. 13d, d'). In P15 mutants, *Barhl1* was expressed in EGL and expanded inwardly from EGL (Fig. 13e, e'). At P21, when no EGL was left in control littermates, *Barhl1* persisted in EGL of the central lobules of the mutant cerebellum (Fig. 13f, f'). The *Barhl1* expression pattern matched that of *Atoh1* in *Neurod1* mutant cerebellum, but with a delay of 1–4 days (Figs. 12, 13).

In summary, the expression of both *Atoh1* and *Barhl1* supports the notion of an expansion of the EGL in lobules VI-VIII and a delayed downregulation of proliferative precursors in these lobules. Because *Atoh1* and *Barhl1* expression remained turned on for a prolonged period in the EGL in order to continue proliferation of the GCPs in *Neurod1* mutant mice, the EGL became thicker in the central lobules compared with lobules IX and X in the same cerebellum (Figs. 7b, 9). The GCs in lobule VIII seemed to lack coordinated migration from EGL to IGL in mutant mice (Fig. 7c).

Discussion

In agreement with our earlier work and that of others (Miyata et al. 1999; Cho and Tsai 2006), we demonstrate that *Neurod1* is indispensible for the differentiation and maintenance of GCs of cerebellar lobules VI-VIII. In contrast to the systemic *Neurod1* null mutant, we have now generated a mouse model in which some lobules develop almost normally, some lobules are consistently agranular, and some lobules show certain GC and PC defects not previously recognized. Our data also suggest that *Neurod1* antagonizes *Atoh1* and thus may aid in moving proliferative GCPs into differentiation.

Lack of *Neurod1* excision in posterior lobules is related to delayed and incomplete *Tg(Atoh1-cre)* expression

In the cerebellum of our conditional *Neurod1* null mouse, we find *Neurod1* mRNA to be present in lobules IX and X, and this lack of *Neurod1* excision is correlated with the inadequate and delayed upregulation of *Tg(Atoh1-cre)* in these lobules. Our data from the other lobules show that *Tg(Atoh1-cre)* can successfully eliminate *Neurod1*, thus indicating the success of the genetic manipulation involved in constructing the floxed *Neurod1*. We also show that, in the cochlear nuclei and spiral sensory neurons of the mutant mice, the expression of *Tg(Atoh1-cre)* is even more delayed compared with *Neurod1* gene upregulation (Kim et al. 2001; Ohyama and Groves 2004), resulting in the continued presence of the *Neurod1* transcript. The molecular mechanism underlying these differences needs further investigation.

Previous studies have shown a gradient of ROSA26-eYFP expression driven by *Tg(Atoh1-cre)*, with YFP expression being high from lobule I through lobule VIII, weak in lobule IX, and almost absent in lobule X (Schuller et al. 2008). This gradient of YFP expression is consistent with the gradient of *Tg(Atoh1-cre)*-mediated ROSA26-LacZ expression shown in our study and thus reflects a consistent expression profile on a different background.

Our observation of cerebellar defects in *Neurod1* conditional null mice is in apparent contrast to that in the normal cerebellum shown in a previous study by using the $GABA_A$ receptor α6 subunit promoter-driving Cre to delete the *Neurod1* gene (Goebbels et al. 2005). However, the $GABA_A$ receptor α6 subunit is expressed only in the post-migratory mature GCs around P14 (Aller et al. 2003). Therefore, deletion of *Neurod1* after the GCs become mature apparently does not interfere with GC viability and produces a near normal cerebellar phenotype. Our data show that posterior lobules develop earlier than the anterior lobules, and that the degree of *Neurod1* dependency is more profound in posterior lobules than in anterior lobules. Combined, our present and previous data suggest that, within each lobule, the susceptibility of GCs to loss of *Neurod1* decreases with the progression of development, leaving the differentiated GCs unaffected by *Neurod1* elimination, but introduces apoptosis if eliminated in postmitotic cells prior to the onset of differentiation. We are currently testing this hypothesis by analyzing the effects of *Neurod1* deletion in a *Pax2-cre* line that shows Cre expression throughout the cerebellum and the ear prior to the upregulation of *Neurod1* (Kim et al. 2001; Ohyama and Groves 2004; Soukup et al. 2009).

Differential defects in cerebellar lobules in *Neurod1* conditional knock-out mice

Previous work on systemic *Neurod1* null mice have shown that the absence of *Neurod1* leads to a lack of foliation and the complete loss of GCs in the posterior half of the cerebellum, whereas a substantial number of GCs survive and differentiate in the anterior lobules (Miyata et al. 1999; Cho and Tsai 2006). Several other studies on mutations involving GC depletion, such as *leaner* and *meander tail* mutations, have also found that the degree of defect in the cerebellum differs considerably between the anterior and posterior lobules with the compartment boundary lying in lobule VI (Herrup and Wilczynski 1982). A gradient of defects in the cerebellar lobules is also observed in medulloblastoma formation. *Olig2*, a bHLH protein, preferentially contributes to GC formation in the posterior lobules of the cerebellum. With conditional overexpression of activated Smoothened under the control of *Olig2*, the mice develop medulloblastoma restricted to the posterior lobules only (Schuller et al. 2008). *Tg(Atoh1-cre)*-driven over-expression of Smoothened or the conditional deletion of the sonic hedgehog receptor Patched is known to produce medulloblastoma followed by severe hyperplasia in the central lobules (Schuller et al. 2008; Yang et al. 2008). Another gene showing a clear delineation of expression is *Tlx3*, which can also result in restricted medulloblastoma (Schuller et al. 2008). Overall, these more recent molecular data indicate a sophisticated molecular subdivision of the cerebellar cortex that may underlie specific targeting of mossy fibers such as the vestibular fibers to the nodulus and uvula (Maklad and Fritzsch 2003).

In our current study, we not only confirm the previous notion of an anterior-posterior differential requirement of *Neurod1* for GC maintenance, but also show that the combination of a delayed posterior upregulation of *Tg(Atoh1-cre)*, combined with the anterior-posterior requirement of *Neurod1*, results in a mosaic of GC developmental loss leading to three distinct areas in the mature cerebellum.

1. Lobules I-V in which some GCs differentiate, and some fail to survive in the absence of *Neurod1*; these lobules nevertheless show a distinct disorganization of PC dendrites into a bipolar pattern that has not previously been reported.
2. Lobules VI-VIII with a near complete loss of all GCs, severe disorganization of PC distribution and dendrites, and diminished foliation.
3. Lobules IX and X with near normal organization of cerebellar architecture and GC development because of the sparing of *Neurod1* recombination.

This newly developed model created by using genetic engineering allows us, for the first time, to investigate GC-dependent aspects of cerebellar cytoarchitecture development that cannot be fully assessed with varied or complete destruction of GCs through other means (Berry and Bradley 1976; Sotelo 1975; Arsenio Nunes et al. 1988). Our model is reproducible and is free of systemic defects that could influence overall viability and thus indirectly affect cerebellar development. Moreover, this is the first model of an agranular cerebellum that provides, in addition to the defective lobules, normal control development in the same animal, albeit in different lobules. Below, we provide an initial assessment of this new model system on hitherto unexplored aspects of the influence of GC axons on PC dendrites and the role of the coordinated transition of bHLH genes for GC proliferation and maturation.

GC survival and differentiation regulate cerebellar layering and PC orientation and distribution

Our data demonstrate, for the first time, that the degree of layer formation is directly tied to the degree of GC differentiation, whereas the normal patterning of PCs depends both on the proper formation of GC axons, the parallel fibers, and on some unrecognized GC properties

dependent on *Neurod1*. In support of this idea, the normal formation of layers is found in lobules I-V and IX-X, but normal PC dendrites exist only in lobules IX and X. Thus, the mere presence of GCs and their parallel fiber axons is necessary for the development of the typical cerebellar layers, but dendritic branching requires additional features that are not provided by the GCs in the *Neurod1*-depleted anterior lobules. This has not previously been noticed, as we and others (Miyata et al. 1999; Cho and Tsai 2006) did not analyze PC development in simple *Neurod1* null mice in sufficient detail.

The absence of any layers and the random distribution of PCs and their dendrites in the poorly defined lobules VI-VIII are consistent with previous work on the function of GCs in agranular cerebella generated by irradiation, viral infection, or GC-specific mutations (Berry and Bradley 1976; Sotelo 1975; Arsenio Nunes et al. 1988). In contrast to those early attempts to identify the developmental significance of GC formation on PC dendritic development, we provide here a model that not only confirms the generality of those findings, but does so with unprecedented reproducibility because it is based on a genetically engineered mouse. We are currently exploring the missing steps in PCs development and their innervations through mossy and climbing fibers, which may also be severely disrupted in their ability to segregate properly to GCs and PCs, respectively (Arsenio Nunes et al. 1988). Should our developmental data confirm previous suggestions (Arsenio Nunes et al. 1988) and show that the segregation of mossy and climbing fibers depends on the presence of GCs and a differential affinity of mossy fibers and climbing fibers to GCs, we should be able to establish the evolution and development of GCs as a central hub for the cerebellum and its development.

In this study, the absence of *Neurod1* severely affects the central lobules, resulting in both GC depletion and PC disorganization. The abnormal arborization of PCs is dependent on GCs, as the degeneration of GCs leads to the abolition of parallel fibers, which, in turn, cannot provide input to the PCs. The monolayer alignment of PCs with the polarity and planar organization of their dendrites perpendicular to parallel fibers represents the functional efficiency implied in central neural tissues, as it allows the maximal divergence and convergence of connections from parallel fibers to PCs.

Some interesting relationships emerge in comparison with existing data. The *Foxp2* missense mutation causes specific language deficiency originally identified in the KE family in which half of the family members have a speech disorder. Fujita et al. (2008) have demonstrated severe ultrasonic vocalization and motor impairment in *Foxp2* knockin mice. They have also found immature development of PCs with poor dendrite formation and overall growth reduction of the cerebellum. In our *Neurod1* conditional null mice, the PC dendrites are disorganized. Further investigations to analyze speech- and language-related impairment by means of our conditional *Neurod1* mouse model are warranted.

Role of bHLH genes in regulation of proliferation and differentiation of neurons

Previous work has shown that many developing systems require the coordinated transition of various bHLH genes with specific aspects of proliferation of neuronal progenitors and their differentiation (Bertrand et al. 2002; Helms et al. 2000). For example, in the ear, the first bHLH gene to be expressed is *Neurog1*. It regulates the proliferation of neuronal precursors, which then differentiate into neurons and hair cells through the upregulation of *Neurod1* or *Atoh1*, respectively (Bulfone et al. 2000; Fritzsch et al. 2006b, 2007; Raft et al. 2007).

In the cerebellum, *Atoh1* functions as a neuronal precursor factor to promote the proliferation of GCPs in the outer EGL (Fig. 14). This is supported by the loss of GC formation in *Atoh1* null mice (Wang et al. 2005;Bermingham et al. 2001) and the additional

precursor proliferation in *Atoh1*-overexpressing mice (Helms et al. 2001). Specifically, overexpression of *Atoh1* causes misregulation of *Neurod1* and other markers of differentiating cerebellar GCs, thus leading to reduced viability of GCs, suggesting that balanced levels of *Atoh1* and some other transcription factors are required for GC development. Our data agree with this scenario, show that normal levels of *Neurod1* are indeed needed for most GC differentiation, and also provide a novel mechanism of regulating *Atoh1* expression to ensure a coordinated transition from an *Atoh1*-positive proliferating neuroblast to a differentiating granule neuron (Fig. 14).

We show here that *Atoh1* is rapidly downregulated when *Neurod1* is upregulated to allow GCPs in the innermost layer of the EGL to differentiate and migrate into their proper topological position in the IGL. In *Neurod1* conditional null mice, the absence of *Neurod1* leads to prolonged expression of *Atoh1* in these precursors, suggesting a negative feedback loop within a given cell as previously suggested for other systems such as the olfactory system (Kawauchi et al. 2004) or the ear (Fritzsch et al. 2006b). Consistent with this idea, we have observed the expansion of *Atoh1* in the inner EGL and continued proliferation of GCPs (as demonstrated by mitotic figures near the ML; Fig. 9c, c'). Because of this delay in turning off *Atoh1* and the absence of *Neurod1* in the central lobules, the migration of GCs is aberrant resulting in their massive degeneration. The precise way that *Atoh1* and *Neurod1* interact with other bHLH genes to regulate both proliferation and differentiation (Barisone et al. 2008) and the specific binding differences that exist in *Atoh1* compared with *Neurod1* in this context remain unclear. However, close examination of the medulloblastoma data base show elevated levels of *Atoh1* and decreased levels of *Neurod1*, consistent with a differential role of those two bHLH genes in mediating either proliferation or differentiation. Recent data on viral-induced overexpression support this notion for *Neurod1* in the hippocampus (Roybon et al. 2009).

Barhl1 is dependent on *Atoh1* expression and lies downstream of *Atoh1* expressed in cerebellar GCs (Chellappa et al. 2008). In our mutant cerebellum, *Barhl1* shows an expansion of its expression similar to that of *Atoh1* expression, as *Atoh1* is a key upstream regulator of *Barhl1*. *Barhl1* expression is maintained longer in the absence of *Neurod1* in the central lobules. In the anterior lobules of the *Neurod1* mutant cerebellum, *Barhl1* may, in part, be responsible for rescuing GCs to some degree. *Barlh1* cannot however save the central lobules. The feedback upregulation of *Atoh1* and *Barhl1* cannot guide the GCs into appropriate migration or differentiation, thereby indicating the critical need of *Neurod1* in these lobules.

In summary, our data on the conditional deletion of *Neurod1* by using the *Tg(Atoh1-cre)* line have generated a novel viable mouse model for the study of agranular cerebellar cortex development. Since only some lobules are massively defective, this model allows intrinsic controls of specific defects within adjacent normally developed lobules. Our data also suggest that *Neurod1* antagonizes *Atoh1* and thus might aid in moving proliferative precursors into differentiation. We are currently testing whether the expression of *Neurod1* under *Atoh1* promoter control can force proliferative GCPs into differentiation as a possible way to combat the fairly frequently occurring childhood tumor medulloblastoma (Fig. 14).

Acknowledgments

We express our thanks to Drs. K.-A. Nave and S. Goebbels, Max-Planck-Institute of Experimental Medicine, for providing the floxed *Neurod1* mice used in this study. We also thank the Bioimaging Facility in the Department of Biology at University of Iowa for assisting with the Leica TCS SP5 confocal microscope. We are grateful to J. Kersigo for extensive help in breeding and genotyping and in the various steps during sample preparation and to K. Thompson for proofreading the manuscript.

This work was supported by an NIH grant (R01 DC 005590) to B.F.

References

Akazawa C, Ishibashi M, Shimizu C, Nakanishi S, Kageyama R. A mammalian helix-loop-helix factor structurally related to the product of *Drosophila* proneural gene *atonal* is a positive transcriptional regulator expressed in the developing nervous system. J Biol Chem 1995;270:8730–8738. [PubMed: 7721778]

Alder J, Cho NK, Hatten ME. Embryonic precursor cells from the rhombic lip are specified to a cerebellar granule neuron identity. Neuron 1996;17:389–399. [PubMed: 8816703]

Alder J, Lee KJ, Jessell TM, Hatten ME. Generation of cerebellar granule neurons in vivo by transplantation of BMP-treated neural progenitor cells. Nat Neurosci 1999;2:535–540. [PubMed: 10448218]

Aller MI, Jones A, Merlo D, Paterlini M, Meyer AH, Amtmann U, Brickley S, Jolin HE, McKenzie AN, Monyer H, Farrant M, Wisden W. Cerebellar granule cell Cre recombinase expression. Genesis 2003;36:97–103. [PubMed: 12820171]

Altman J, Bayer SA. Prenatal development of the cerebellar system in the rat. I. Cytogenesis and histogenesis of the deep nuclei and the cortex of the cerebellum. J Comp Neurol 1978;179:23–48. [PubMed: 8980716]

Arsenio Nunes ML, Sotelo C, Wehrle R. Organization of spinocerebellar projection map in three types of agranular cerebellum: Purkinje cells vs. granule cells as organizer element. J Comp Neurol 1988;273:120–136. [PubMed: 2463274]

Barisone GA, Yun JS, Diaz E. From cerebellar proliferation to tumorigenesis: new insights into the role of Mad3. Cell Cycle 2008;7:423–427. [PubMed: 18235219]

Ben-Arie N, McCall AE, Berkman S, Eichele G, Bellen HJ, Zoghbi HY. Evolutionary conservation of sequence and expression of the bHLH protein Atonal suggests a conserved role in neurogenesis. Hum Mol Genet 1996;5:1207–1216. [PubMed: 8872459]

Ben-Arie N, Bellen HJ, Armstrong DL, McCall AE, Gordadze PR, Guo Q, Matzuk MM, Zoghbi HY. Math1 is essential for genesis of cerebellar granule neurons. Nature 1997;390:169–172. [PubMed: 9367153]

Benediktsson AM, Schachtele SJ, Green SH, Dailey ME. Ballistic labeling and dynamic imaging of astrocytes in organotypic hippocampal slice cultures. J Neurosci Methods 2005;141:41–53. [PubMed: 15585287]

Bermingham NA, Hassan BA, Wang VY, Fernandez M, Banfi S, Bellen HJ, Fritzsch B, Zoghbi HY. Proprioceptor pathway development is dependent on Math1. Neuron 2001;30:411–422. [PubMed: 11395003]

Berry M, Bradley P. The growth of the dendritic trees of Purkinje cells in irradiated agranular cerebellar cortex. Brain Res 1976;116:361–387. [PubMed: 974782]

Bertrand N, Castro DS, Guillemot F. Proneural genes and the specification of neural cell types. Nat Rev Neurosci 2002;3:517–530. [PubMed: 12094208]

Bradley P, Berry M. The Purkinje cell dendritic tree in mutant mouse cerebellum. A quantitative Golgi study of Weaver and Staggerer mice. Brain Res 1978;142:135–141. [PubMed: 75044]

Bulfone A, Menguzzato E, Broccoli V, Marchitiello A, Gattuso C, Mariani M, Consalez GG, Martinez S, Ballabio A, Banfi S. *Barhl1*, a gene belonging to a new subfamily of mammalian homeobox genes, is expressed in migrating neurons of the CNS. Hum Mol Genet 2000;9:1443–1452. [PubMed: 10814725]

Buratowski S. Transcription. Gene expression—where to start? Science 2008;322:1804–1805. [PubMed: 19095933]

Chellappa R, Li S, Pauley S, Jahan I, Jin K, Xiang M. Barhl1 regulatory sequences required for cell-specific gene expression and autoregulation in the inner ear and central nervous system. Mol Cell Biol 2008;28:1905–1914. [PubMed: 18212062]

Cho JH, Tsai MJ. Preferential posterior cerebellum defect in BETA2/NeuroD1 knockout mice is the result of differential expression of BETA2/NeuroD1 along anterior-posterior axis. Dev Biol 2006;290:125–138. [PubMed: 16368089]

Dahmane N, Ruiz-i-Altaba A. Sonic hedgehog regulates the growth and patterning of the cerebellum. Development 1999;126:3089–3100. [PubMed: 10375501]

del Cerro M, Cogen J, Cerro C. Stevenel's blue, an excellent stain for optical microscopical study of plastic embedded tissues. Microsc Acta 1980;83:117–121. del. [PubMed: 6156384]

Dino MR, Willard FH, Mugnaini E. Distribution of unipolar brush cells and other calretinin immunoreactive components in the mammalian cerebellar cortex. J Neurocytol 1999;28:99–123. [PubMed: 10590511]

Englund C, Kowalczyk T, Daza RA, Dagan A, Lau C, Rose MF, Hevner RF. Unipolar brush cells of the cerebellum are produced in the rhombic lip and migrate through developing white matter. J Neurosci 2006;26:9184–9195. [PubMed: 16957075]

Fritzsch B, Muirhead KA, Feng F, Gray BD, Ohlsson-Wilhelm BM. Diffusion and imaging properties of three new lipophilic tracers, NeuroVue Maroon, NeuroVue Red and NeuroVue Green and their use for double and triple labeling of neuronal profile. Brain Res Bull 2005;66:249–258. [PubMed: 16023922]

Fritzsch B, Pauley S, Feng F, Matei V, Nichols DH. The evolution of the vertebrate auditory system: transformations of vestibular mechanosensory cells for sound processing is combined with newly generated central processing neurons. Int J Comp Psychol 2006a;19:1–24.

Fritzsch B, Pauley S, Beisel KW. Cells, molecules and morphogenesis: the making of the vertebrate ear. Brain Res 2006b;1091:151–171. [PubMed: 16643865]

Fritzsch B, Beisel KW, Pauley S, Soukup G. Molecular evolution of the vertebrate mechanosensory cell and ear. Int J Dev Biol 2007;51:663–678. [PubMed: 17891725]

Fujita, S. Autoradiographic studies on histogenesis of the cerebellar cortex. In: Llinas, R., editor. Neurobiology of cerebellar evolution and development. American Medical Association; Chicago: 1969. p. 743-747.

Fujita S, Shimada M, Nakamura T. H^3-thymidine autoradiographic studies on the cell proliferation and differentiation in the external and the internal granular layers of the mouse cerebellum. J Comp Neurol 1966;128:191–208. [PubMed: 5970298]

Fujita E, Tanabe Y, Shiota A, Ueda M, Suwa K, Momoi MY, Momoi T. Ultrasonic vocalization impairment of Foxp2 (R552H) knockin mice related to speech-language disorder and abnormality of Purkinje cells. Proc Natl Acad Sci USA 2008;105:3117–3122. [PubMed: 18287060]

Gazit R, Krizhanovsky V, Ben-Arie N. Math1 controls cerebellar granule cell differentiation by regulating multiple components of the Notch signaling pathway. Development 2004;131:903–913. [PubMed: 14757642]

Goebbels S, Bode U, Pieper A, Funfschilling U, Schwab MH, Nave KA. Cre/loxP-mediated inactivation of the bHLH transcription factor gene *NeuroD/BETA2*. Genesis 2005;42:247–252. [PubMed: 16028233]

Goldowitz D, Hamre K. The cells and molecules that make a cerebellum. Trends Neurosci 1998;21:375–382. [PubMed: 9735945]

Gurung B, Fritzsch B. Time course of embryonic midbrain and thalamic auditory connection development in mice as revealed by carbocyanine dye tracing. J Comp Neurol 2004;479:309–327. [PubMed: 15457503]

Hatten ME, Heintz N. Mechanisms of neural patterning and specification in the developing cerebellum. Annu Rev Neurosci 1995;18:385–408. [PubMed: 7605067]

Hatten ME, Furie MB, Rifkin DB. Binding of developing mouse cerebellar cells to fibronectin: a possible mechanism for the formation of the external granular layer. J Neurosci 1982;2:1195–1206. [PubMed: 6288895]

Helms AW, Abney AL, Ben-Arie N, Zoghbi HY, Johnson JE. Autoregulation and multiple enhancers control Math1 expression in the developing nervous system. Development 2000;127:1185–1196. [PubMed: 10683172]

Helms AW, Gowan K, Abney A, Savage T, Johnson JE. Overexpression of MATH1 disrupts the coordination of neural differentiation in cerebellum development. Mol Cell Neurosci 2001;17:671–682. [PubMed: 11312603]

Herrup K, Wilczynski SL. Cerebellar cell degeneration in the leaner mutant mouse. Neuroscience 1982;7:2185–2196. [PubMed: 7145091]

Higashijima S, Michiue T, Emori Y, Saigo K. Subtype determination of *Drosophila* embryonic external sensory organs by redundant homeo box genes *BarH1* and *BarH2*. Genes Dev 1992;6:1005–1018. [PubMed: 1350558]

Hoshino M, Nakamura S, Mori K, Kawauchi T, Terao M, Nishimura YV, Fukuda A, Fuse T, Matsuo N, Sone M, Watanabe M, Bito H, Terashima T, Wright CV, Kawaguchi Y, Nakao K, Nabeshima Y. *Ptf1a*, a bHLH transcriptional gene, defines GABAergic neuronal fates in cerebellum. Neuron 2005;47:201–213. [PubMed: 16039563]

Isaka F, Ishibashi M, Taki W, Hashimoto N, Nakanishi S, Kageyama R. Ectopic expression of the bHLH gene *Math1* disturbs neural development. Eur J Neurosci 1999;11:2582–2588. [PubMed: 10383648]

Jensen-Smith H, Gray B, Muirhead K, Ohlsson-Wilhelm B, Fritzsch B. Long-distance three-color neuronal tracing in fixed tissue using NeuroVue dyes. Immunol Invest 2007;36:763–789. [PubMed: 18161528]

Joyner AL, Zervas M. Genetic inducible fate mapping in mouse: establishing genetic lineages and defining genetic neuroanatomy in the nervous system. Dev Dyn 2006;235:2376–2385. [PubMed: 16871622]

Kageyama R, Ohtsuka T, Kobayashi T. The *Hes* gene family: repressors and oscillators that orchestrate embryogenesis. Development 2007;134:1243–1251. [PubMed: 17329370]

Kawauchi S, Beites CL, Crocker CE, Wu HH, Bonnin A, Murray R, Calof AL. Molecular signals regulating proliferation of stem and progenitor cells in mouse olfactory epithelium. Dev Neurosci 2004;26:166–180. [PubMed: 15711058]

Kim WY, Fritzsch B, Serls A, Bakel LA, Huang EJ, Reichardt LF, Barth DS, Lee JE. NeuroD-null mice are deaf due to a severe loss of the inner ear sensory neurons during development. Development 2001;128:417–426. [PubMed: 11152640]

Kojima T, Ishimaru S, Higashijima S, Takayama E, Akimaru H, Sone M, Emori Y, Saigo K. Identification of a differenttype homeobox gene, *BarH1*, possibly causing Bar (B) and Om (1D) mutations in *Drosophila*. Proc Natl Acad Sci USA 1991;88:4343–4347. [PubMed: 1674606]

Larramendi, L. Analysis of synaptogenesis in the cerebellum of the mouse. In: Llinas, R., editor. Neurobiology of cerebellar evolution and development. American Medical Association; Chicago: 1969. p. 803-843.

Lee JE. Basic helix-loop-helix genes in neural development. Curr Opin Neurobiol 1997;7:13–20. [PubMed: 9039799]

Lee JE, Hollenberg SM, Snider L, Turner DL, Lipnick N, Weintraub H. Conversion of *Xenopus* ectoderm into neurons by NeuroD, a basic helix-loop-helix protein. Science 1995;268:836–844. [PubMed: 7754368]

Lee JK, Cho JH, Hwang WS, Lee YD, Reu DS, Suh-Kim H. Expression of neuroD/BETA2 in mitotic and postmitotic neuronal cells during the development of nervous system. Dev Dyn 2000;217:361–367. [PubMed: 10767080]

Leung C, Lingbeek M, Shakhova O, Liu J, Tanger E, Saremaslani P, Van Lohuizen M, Marino S. Bmi1 is essential for cerebellar development and is overexpressed in human medulloblastomas. Nature 2004;428:337–341. [PubMed: 15029199]

Li S, Price SM, Cahill H, Ryugo DK, Shen MM, Xiang M. Hearing loss caused by progressive degeneration of cochlear hair cells in mice deficient for the *Barhl1* homeobox gene. Development 2002;129:3523–3532. [PubMed: 12091321]

Li S, Qiu F, Xu A, Price SM, Xiang M. Barhl1 regulates migration and survival of cerebellar granule cells by controlling expression of the *neurotrophin-3* gene. J Neurosci 2004;24:3104–3114. [PubMed: 15044550]

Ma Q, Chen Z, Barco Barrantes I, Pompa JL, Anderson DJ. Neurogenin1 is essential for the determination of neuronal precursors for proximal cranial sensory ganglia. Neuron 1998;20:469–482. del. de la. [PubMed: 9539122]

Machold R, Fishell G. Math1 is expressed in temporally discrete pools of cerebellar rhombic-lip neural progenitors. Neuron 2005;48:17–24. [PubMed: 16202705]

Maklad A, Fritzsch B. Partial segregation of posterior crista and saccular fibers to the nodulus and uvula of the cerebellum in mice, and its development. Brain Res Dev Brain Res 2003;140:223–236.

Matei V, Pauley S, Kaing S, Rowitch D, Beisel KW, Morris K, Feng F, Jones K, Lee J, Fritzsch B. Smaller inner ear sensory epithelia in *Neurog1* null mice are related to earlier hair cell cycle exit. Dev Dyn 2005;234:633–650. [PubMed: 16145671]

Matei VA, Feng F, Pauley S, Beisel KW, Nichols MG, Fritzsch B. Near-infrared laser illumination transforms the fluorescence absorbing X-Gal reaction product BCI into a transparent, yet brightly fluorescent substance. Brain Res Bull 2006;70:33–43. [PubMed: 16750480]

Miale IL, Sidman RL. An autoradiographic analysis of histogenesis in the mouse cerebellum. Exp Neurol 1961;4:277–296. [PubMed: 14473282]

Miyata T, Maeda T, Lee JE. NeuroD is required for differentiation of the granule cells in the cerebellum and hippocampus. Genes Dev 1999;13:1647–1652. [PubMed: 10398678]

Mugnaini, E. Ultrastructural studies on the cerebellar histogenesis. II. Maturation of nerve cell populations and establishment of synaptic connections in the cerebellar cortex of the chick. In: Llinas, R., editor. Neurobiology of cerebellar evolution and development. American Medical Association; Chicago: 1969. p. 749-782.

Mugnaini E, Dino MR, Jaarsma D. The unipolar brush cells of the mammalian cerebellum and cochlear nucleus: cytology and microcircuitry. Prog Brain Res 1997;114:131–150. [PubMed: 9193142]

Ohyama T, Groves AK. Generation of Pax2-Cre mice by modification of a Pax2 bacterial artificial chromosome. Genesis 2004;38:195–199. [PubMed: 15083520]

Raft S, Koundakjian EJ, Quinones H, Jayasena CS, Goodrich LV, Johnson JE, Segil N, Groves AK. Cross-regulation of Ngn1 and Math1 coordinates the production of neurons and sensory hair cells during inner ear development. Development 2007;134:4405–4415. [PubMed: 18039969]

Roybon L, Hjalt T, Stott S, Guillemot F, Li JY, Brundin P. Neurogenin2 directs granule neuroblast production and amplification while NeuroD1 specifies neuronal fate during hippocampal neurogenesis. PLoS ONE 2009;4:e4779. [PubMed: 19274100]

Schuller U, Heine VM, Mao J, Kho AT, Dillon AK, Han YG, Huillard E, Sun T, Ligon AH, Qian Y, Ma Q, Alvarez-Buylla A, McMahon AP, Rowitch DH, Ligon KL. Acquisition of granule neuron precursor identity is a critical determinant of progenitor cell competence to form Shh-induced medulloblastoma. Cancer Cell 2008;14:123–134. [PubMed: 18691547]

Sgaier SK, Millet S, Villanueva MP, Berenshteyn F, Song C, Joyner AL. Morphogenetic and cellular movements that shape the mouse cerebellum; insights from genetic fate mapping. Neuron 2005;45:27–40. [PubMed: 15629700]

Sotelo C. Anatomical, physiological and biochemical studies of the cerebellum from mutant mice. II. Morphological study of cerebellar cortical neurons and circuits in the weaver mouse. Brain Res 1975;94:19–44. [PubMed: 1148865]

Sotelo C. Viewing the cerebellum through the eyes of Ramon y Cajal. Cerebellum 2008;7:517–522. [PubMed: 18972180]

Soukup GA, Fritzsch B, Pierce ML, Weston MD, Jahan I, McManus MT, Harfe BD. Residual microRNA expression dictates the extent of inner ear development in conditional Dicer knockout mice. Dev Biol 2009;328:328–341. [PubMed: 19389351]

Voogd J, Glickstein M. The anatomy of the cerebellum. Trends Neurosci 1998;21:370–375. [PubMed: 9735944]

Wang VY, Rose MF, Zoghbi HY. Math1 expression redefines the rhombic lip derivatives and reveals novel lineages within the brainstem and cerebellum. Neuron 2005;48:31–43. [PubMed: 16202707]

Weiss GM, Pysh JJ. Evidence for loss of Purkinje cell dendrites during late development: a morphometric Golgi analysis in the mouse. Brain Res 1978;154:219–230. [PubMed: 687992]

Yang ZJ, Ellis T, Markant SL, Read TA, Kessler JD, Bourboulas M, Schuller U, Machold R, Fishell G, Rowitch DH, Wainwright BJ, Wechsler-Reya RJ. Medulloblastoma can be initiated by deletion of Patched in lineage-restricted progenitors or stem cells. Cancer Cell 2008;14:135–145. [PubMed: 18691548]

Zebedee Z, Hara E. Id proteins in cell cycle control and cellular senescence. Oncogene 2001;20:8317–8325. [PubMed: 11840324]

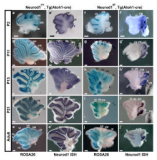

Fig. 1.

Inadequate *Tg(Atoh1-cre)* upregulation revealed by ROSA26 (**a-e**, **f-j**) failed to excise *Neurod1* mRNA (**a'-e'**, **f'-j'**) in lobule IX and X in *Neurod1* mutant cerebellum revealed by in situ hybridization of *Neurod1*. **a-e'** *Neurod1*$^{f/+}$, *Tg(Atoh1-cre)[control]*. **f-j'** *Neurod1*$^{f/f}$, *Tg(Atoh1-cre)[mutant]*. **a**, **f** In P2 control and mutant cerebella, *Tg(Atoh1cre)* was prominently expressed from lobule I to VIII, weakly expressed in lobule IX in heterozygous, but completely absent in lobule X. **b**, **g** *Tg(Atoh1-cre)* expression progressed further to lobule IX by P11 and was homogeneously expressed in heterozygous cerebellum but misplaced and condensed in EGL of central lobules in mutant cerebellum. **c**, **h** *Tg(Atoh1-cre)* was expressed uniformly in up to one third of lobule X by P15 in heterozygous cerebellum and dispersed in central lobules in mutant cerebellum. **d**, **i**, **e**, **j** *Tg(Atoh1-cre)* expression progressed to half of lobule X in P21 and in adult heterozygous cerebellum (**d**, **e**) and was lost in central lobules in mutants (**i**, **j**). **a'-e'** *Neurod1* was expressed uniformly in all the lobules in heterozygous cerebellum as shown by in situ hybridization of *Neurod1*. **f'-j'** Expression of *Neurod1* was absent in lobules I to half of VIII in mutant from P2 to adult when *Tg(Atoh1-cre)* upregulation was prominent. Despite the late upregulation in lobule IX and X, *Tg(Atoh1-cre)* failed to excise *Neurod1* in lobules X, IX, and 1/2VIII in mutant cerebellum. The recombination of *Neurod1* by using *Tg(Atoh1-cre)* must happen in embryonic stages and results in no apparent additional recombination after further upregulation of *Tg(Atoh1-cre*) as revealed by the expansion of ROSA26-lacZ. **h'**, **i'** *Boxed regions* are shown at higher magnification in **h"**, **i"**, respectively. *Bars* 250 μm (**a-j**, **a'-j'**), 10 μm (**h"**, **i"**)

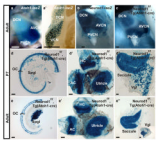

Fig. 2.

Expression of *Tg(Atoh1-cre)* and *Neurod1* in the cochlear nucleus and in inner ear sensory neurons with inadequate upregulation of *Tg(Atoh1-cre)* consistent with normal development of cochlear nucleus and inner ear in *Neurod1* conditional null mice. **a-a'** *Atoh1* was strongly expressed in both dorsal and ventral cochlear nucleus in adults as shown by lacZ expression. **b** *Neurod1* was also expressed in both cochlear nuclei more prominently in dorsal cochlear nucleus as revealed by lacZ. **c** However, the cochlear nucleus developed normally in the absence of *Neurod1*, as shown in *Neurod1* conditional null mice. **d-d"** *Tg(Atoh1-cre)* expression in spiral ganglia revealed by ROSA26 was insufficient and delayed as shown in P7 *Neurod1* conditional null mice. **e-e"** Inner ear sensory neurons were normal as shown by ROSA26 in mutant mice. Note that ROSA26 shows lacZ for all of past and present *Atoh1* upregulation. In contrast, *Atoh1*-lacZ and *Neurod1*-lacZ show only actual expression of *Atoh1* and *Neurod1*, respectively (*DCN* dorsal cochlear nucleus, *AVCN* antero-ventral cochlear nucleus, *PVCN* postero-ventral cochlear nucleus, *Spgl* spiral ganglion, *OC* organ of Corti, *HC* horizontal crista, *AC* anterior crista, *Vgl* vestibular ganglion). *Bars* 100 μm (**a**, **a'**, **d-e"**), 250 μm (**b**, **c**)

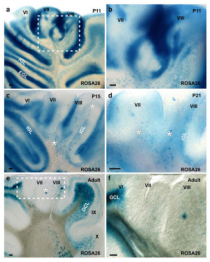

Fig. 3.

Absence of *Neurod1* led to massive loss of granule cells (GCs) in the central lobules of *Neurod1* mutant cerebellum. **a**, **b** GCs shown by ROSA26 were abnormally shifted from the external granular layer (*EGL*) to the internal granular layer (*IGL*) in central lobules (half of *VI-VIII*) in P11 *Neurod1* mutant cerebellum, whereas GCs were almost normally organized in EGL and IGL in other lobules (*boxed area* in **a** shown at higher magnification in **b**). **c** By P15, GCs were dispersed and scattered from EGL to IGL in central lobules (*asterisks*). **d** At P21, the majority of GCs were lost in lobule VII and half of lobule VIII (*asterisks*). **e**, **f** Almost all the GCs were lost in central lobules in adult (asterisks; *GCL* granule cell layer; *boxed area* in **e** shown at higher magnification in **f**). *Bars* 100 μm

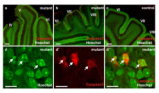

Fig. 4.

Granule cells (GCs) degenerate via apoptotic cell death in the absence of *Neurod1*, as demonstrated by activated caspase 3 staining in P11 mice. **a** GC losses were partial in the anterior lobules of *Neurod1* mutant cerebellum with few activated caspase-3-positive cells, as shown by caspase 3 antibody staining. **b**, **d-d”** Severe degeneration of GCs occurred in the central lobules of *Neurod1* mutant cerebellum analyzed by appearance of pyknotic nuclei shown with Hoechst stain. Such apoptotic cells showed co-localization (*arrows*) with the activated caspase 3 (**d”**). **c** Occasional caspase-3-positive cells were present in the *Neurod1* heterozygous cerebellum. *Bars* 100 μm (**a-c**), 10 μm (**d-d”**)

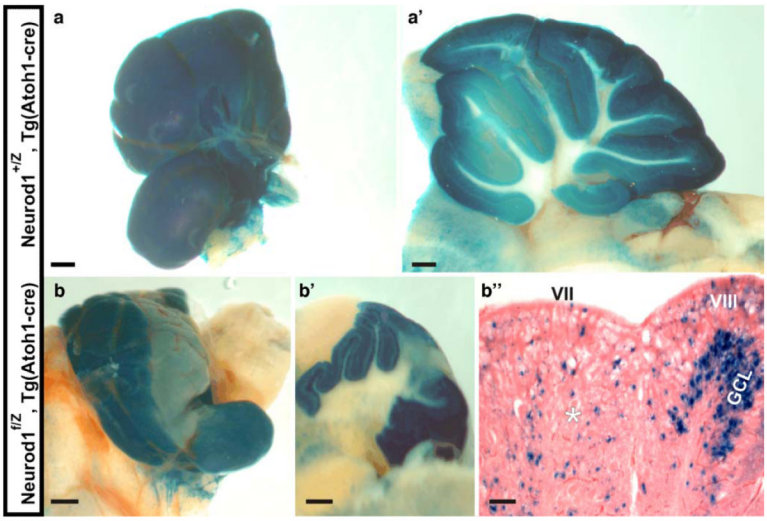

Fig. 5.

Loss of granule cells in the central lobules of adult *Neurod1*$^{f/z}$, *Tg(Atoh1-cre)* mice observed by *Neurod1*-lacZ expression. **a**, **a'** *Neurod1-lacZ* was expressed uniformly in all the lobules in heterozygous [*Neurod1*$^{+/Z}$, *Tg(Atoh1-cre)*] cerebellum. **b-b"** Granule cell loss demonstrated by the absence of *Neurod1*-lacZ expression in the central lobules in *Neurod1*$^{f/Z}$ mice, which carry *Neurod1* null allele containing the *lacZ* reporter gene in place of the *Neurod1* coding region (*GCL* granule cell layer). Note that the lacZ expression reflects endogenous *Neurod1* expression. Almost all the granule cells were lost in lobule VII (*asterisk* in **b"**). *Bars* 10 μm (**a-b'**), 50 μm (**b"**)

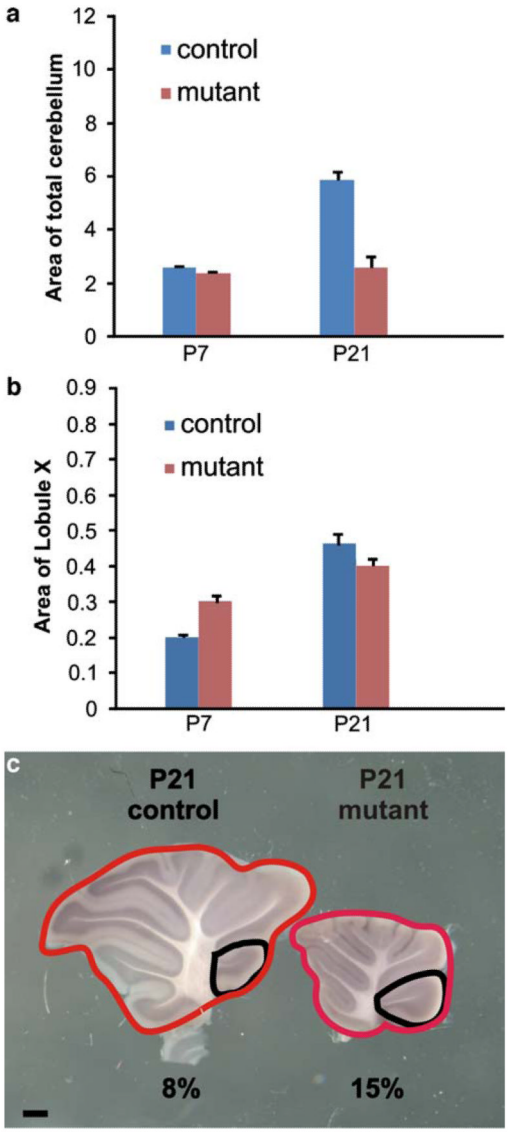

Fig. 6.

Normal growth of lobule-X in *Neurod1* mutant cerebellum in comparison with other lobules. **a** Area of near mid-sagittal sections was measured by using Image-Pro in P7 and P21 in *Neurod1* heterozygous and mutant cerebellum. The area in the mutant was comparable with in heterozygotes at P7 but drastically reduced by P21. **b** Area measurement of lobule X showed higher growth in mutant than heterozygous cerebellum at P7, but at P21, the growth reduced slightly in mutant compared with heterozygous cerebellum. **c** Percentage of growth of lobule X compared with that of total cerebellum was greatly increased in the mutant and was almost double in mutant compared with heterozygous P21 cerebellum. The presence of *Neurod1* in lobule IX and X rescued normal growth, whereas absence of *Neurod1* caused a massive size reduction in the other lobules of the mutant cerebellum. *Bar* 250 μm

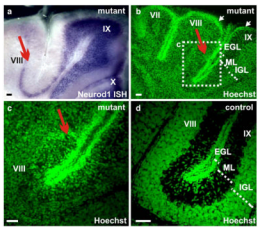

Fig. 7.

Presence of *Neurod1* rescued the posterior lobules in *Neurod1* conditional mutant cerebellum, as shown in P15 mice. **a** Retention of *Neurod1* in the posterior lobules (1/2VIII-X) of *Neurod1* conditional null mice, as shown by in situ hybridization of *Neurod1*. **b** EGL was thicker in central lobules compared with that of lobules IX and X, as shown by Hoechst stain (*white arrows*). The *boxed area* in **b** is shown at higher magnification in **c** (*EGL* external granular layer, *ML* molecular layer, *IGL* internal granular layer). **c** In mutants, migration of GCs was dispersed and scattered from EGL to IGL in central lobules starting from the point (*red arrow* in **c**) in lobule VIII from which the *Neurod1* gene was excised (*red arrow* in **a**). The layers of cerebellum were severely disorganized in central lobules in the mutant (**b**), whereas in posterior lobules of same cerebellum (**b**), they were arranged in a pattern similar to heterozygous cerebellum (**d**). *Bars* 50 μm

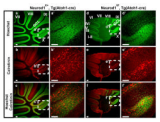

Fig. 8.

Absence of *Neurod1* caused reduction of GCs in the anterior lobules but normal organization of UBCs in *Neurod1* conditional null cerebellum, as shown by Hoechst and calretinin staining, respectively, in adult mice. **a**, **a'** Normal organization and equal distribution of GCs along all the lobules in heterozygous cerebellum, as shown by Hoechst stain. **d**, **d'** Density of GCs in lobules 1/2VIII-X was comparable with heterozygous cerebellum, whereas there was partial loss of GCs in the anterior lobules (I-1/2VI) and severe loss in central lobules (1/2VI-1/2VIII). **b-c'** Abundant UBCs were found only in lobules X and half of IX in heterozygous cerebellum shown by calretinin staining (*red*). **e-f'** UBCs were normally distributed in lobules X and half of IX in mutant cerebellum with no defect attributable to retention of *Neurod1* in these lobules with rescued normal morphology. Note that the mutant cerebellum section lies near the hemispheres resulting in a smaller size of all lobules (*boxed areas* in **a-f** shown at higher magnification in **a'–f'**). *Bars* 100 μm

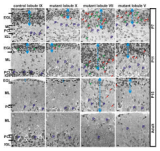

Fig. 9.

Changes in the different layers in the different lobules over time, as shown by Stevenel's staining. **a-a"'** All the layers of the cerebellum were distinct and well organized in control mice, as shown in lobule IX in which the thickness (*blue arrow*) of the external granular layer (*EGL*), and numbers of GC were reduced linearly with progression of age (*ML* molecular layer, *PCL* Purkinje cell layer, *IGL* internal granular layer). **b-b"'** In lobule X of mutant cerebellum, all the layers were organized normally at all ages. **c-c"'** In central lobules shown in lobule VII of *Neurod1* mutant cerebellum, the EGL was expanded (*blue arrow*), and the number of GCs were abnormally increased in P11 (**c'**) from P7 (**c**), although by P15, GCs were dispersed and scattered and many pyknotic nuclei (*red arrows*) and mitotic nuclei (*green arrowheads*) were observed in lobule VII, with no ML and no definite PCL (*P*). **d-d"'** In the anterior lobules shown in lobule V of *Neurod1* mutant mice, the layers were reasonably well-organized, but pyknotic nuclei and mitotic nuclei were observed in EGL in P7 and P11 mice (**d**, **d'**). *Bars* 10 μm

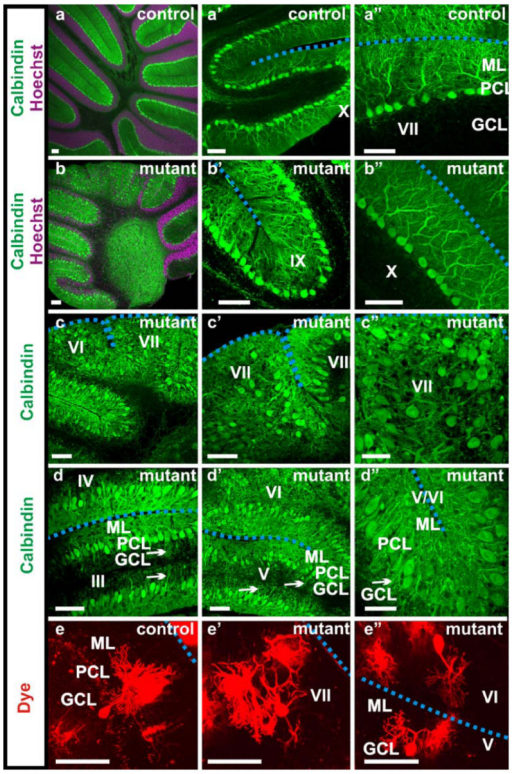

Fig. 10.

Aberration of Purkinje cell (PC) dendrites was directly proportional to granule cell loss in *Neurod1* conditional mutant cerebellum, as shown by calbindin staining (**a-d”**) and dye tracing (**e-e”**) in adult mice (*ML* molecular layer, *PCL* PC layer, *GCL* granule cell layer). **a-a”**, **e** PCs were oriented in a monolayer with nicely organized dendrites in ML throughout all the lobules in control cerebellum. **b-b”** In *Neurod1* mutant cerebellum, normal organization of PCs were observed only in lobules X and IX, where PCs were arranged in a single layer, and their dendrites projected toward the ML. **c-c”**, **e’** In the central lobules (1/2VI-1/2VIII) of mutant cerebellum, PCs were randomly organized with no specific direction of their dendrites. **d-d”**, **e”** In the anterior lobules (I-1/2VI) of mutant cerebellum, PCs almost formed a single layer, but their dendrites were either inversely polarized (*arrow*) toward GCL or Bifurcated and bidirectional (**e”**) to both the pial surface (*dotted blue line*) and GCL. *Bars* 100 μm (**a-b’**, **c-c’**, **d-d’**), 50 μm (**c”**, **d”**), 10 μm (**e-e”**)

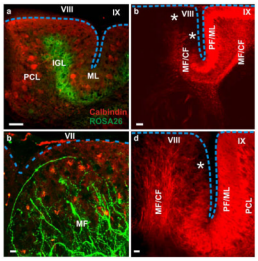

Fig. 11.

Distribution of mossy fibers affected by GC loss in central lobules of mutant cerebellum, as shown in adult mice by lipophilic dye tracing. **a** Distribution of PCs and GCs in lobule VIII of mutant cerebellum shown by calbindin staining and ROSA26, respectively (*ML* molecular layer, *IGL* internal granular layer, *PCL* Purkinje cell layer). **b-d** Mossy fibers (*MF*) in the central lobules directly pass toward the pial surface (*dotted blue line*) instead of synapsing with the GCs because of the nonexistence of the latter (*CF* climbing fiber, *PF* parallel fiber). Moreover, parallel fibers could not be traced in the central lobule consistent with GC loss (*asterisk*). *Bars* 50 μm (**a**, **c**), 20 μm (**d**), 10 μm (**b**)

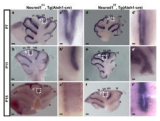

Fig. 12.

Atoh1 expression started normally but expanded and stayed turned on for longer in *Neurod1* mutant cerebellum, as shown by in situ hybridization of *Atoh1*. **a–b'** *Atoh1* was expressed in the outer EGL with a gradient that was higher in the anterior lobules than in the posterior lobules at P7 and P11 heterozygous mice. **c**, **c'** By P15, *Atoh1* expression was abolished in almost all lobules, except for some retention in lobule VII in heterozygous mice. **d**, **d'** In P7 *Neurod1* mutant cerebellum, *Atoh1* was expressed in a similar pattern as that in P7 heterozygous cerebellum. **e**, **e'** In the P11 mutant, *Atoh1* was abnormally expanded inwardly toward the inner EGL and IGL in the central lobules. **f**, **f'** *Atoh1* expression was still maintained in P15 mutant cerebellum, with the gradient being higher in the anterior and central lobules and almost diminished in lobules IX and X. The *boxed areas* in **a-f** are shown at higher magnification in **a'-f'**. *Bars* 250 μm (**a-f**), 50 μm (**a'-f'**)

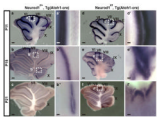

Fig. 13.

Spatial and temporal expression of *Barhl1* changes in absence of *Neurod1* in cerebellum, as shown by in situ hybridization of *Barhl1*. **a**, **a'** *Barhl1* was expressed in EGL in all lobules and in IGL, was highly expressed in anterior lobules I-1/2VI, absent in lobules VII and VIII, and low in lobules IX and X in P11 heterozygous cerebellum. **b-b"** By P15, *Barhl1* expression was downregulated in IGL and EGL in heterozygous cerebellum. **c** By P21, *Barhl1* expression was diminished in heterozygous mice. **d**, **d'** In P11 mutant cerebellum, IGL was almost devoid of *Barhl1* expression, except for some in lobule X; EGL showed expanded *Barhl1* expression. **e**, **e'** *Barhl1* expression persisted and expanded in EGL predominantly in central lobules in mutant P15 cerebellum, instead of being expressed in IGL. **f**, **f'** *Barhl1* abnormally continued to be expressed in EGL of central lobules in P21 mutant cerebellum. The *boxed areas* in **a-f** are shown at higher magnification in **a'-f'**. *Bars* 250 μm (**a-f**), 50 μm (**a'-f'**, **b"**)

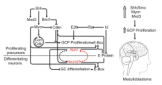

Fig. 14.

Differential control of granule cell progenitor (*GCP*) proliferation and differentiation in cerebellar development and tumorigenesis. Overview of the signaling pathways for proliferation and differentiation of the GCP from neural stem cells. *Atoh1* expressed in GCP promotes GCP proliferation, whereas *Neurod1* facilitates GC differentiation, both by forming heterodimers with ubiquitously expressed E proteins and activating downstream E-box-containing genes. Our data suggest that *Neurod1* regulates *Atoh1* via a negative feedback loop. After upregulation of *Neurod1*, *Atoh1* shuts down, thereby promoting transition from proliferation to differentiation. In the absence of *Neurod1*, continued expression of *Atoh1* causes enhanced proliferation of GCP, aberrant migration, and failure of differentiation, eventually leading to extensive cell death. Sonic hedgehog (*Shh*) plays a key role in GCP proliferation by positively regulating cyclin D1 and cyclin D2 and by inducing expression of Mycn, Mxd3 and Bmi1. Overexpression of Shh and its receptor Smoothened (*Smo*), Mycn, or Mxd3 gives rise to the uncontrolled proliferation of GCP and the formation of medulloblastoma (Schuller et al. 2008; Yang et al. 2008). Id proteins also affect the balance between proliferation and differentiation by binding to and inhibiting bHLH proteins and also by binding to retinoblastoma (*Rb*) proteins, key regulators of cell cycle progression (Zebedee and Hara 2001)

Table 1

Overall growth and pancreas function are normal in *Neurod1* conditional knock-out mice

Age (weeks)	*Neurod1*$^{f/+}$,*Tg(Atoh1-cre)*		*Neurod1*$^{f/f}$,*Tg(Atoh1-cre)*	
	Body weight (g)	**Blood glucose (mg/dl)**	**Body weight (g)**	**Blood glucose (mg/dl)**
1	4.4	102	4.3	97
2	7.9	119	7.7	121
3	10	136	8.8	115
4	18.1	172	16.4	186
5	23.1	136	21.6	134
6	19.3	134	21.5	131

Table 2

Proliferative and degenerative changes in EGL in various lobules of cerebellum in *Neurod1* conditional mutant [*Neurod1*$^{f/f}$,*Tg(Atoh1-cre)*] and control [*Neurod1*$^{f/+}$,*Tg(Atoh1-cre)*] mice

Age	Control L-IX		Mutant L-X		Mutant L-VII		Mutant L-V	
	Mean	SD	Mean	SD	Mean	SD	Mean	SD
Thickness of EGL (μm)								
P7	78	2	50	3	75	13	82	3
P11	48	1	30	2	98	23	55	2
P15	10	2	13	3	42	6	34	13
Number of GCs in EGL (in 40-μm region)								
P7	31	5	27	3.6	15	0.6	29	3.1
P11	28	3	20	2.5	30	6	17	2.1
P15	8	0.6	7	1.2	13	1.2	8	3.8
Number of pyknotic cells in EGL (in 40-μm region)								
P7	1	1	1	1	7	0.6	0.7	1.2
P11	0	0	0.3	0.6	4.3	1.5	2.3	1.5
P15	0	0	0	0	1	1	1	1
Number of mitotic cells in EGL (in 40-μm region)								
P7	1.7	1.5	1	1	2.7	1.2	1.3	0.6
P11	0.7	0.6	1	0	2.7	2.1	1.3	0.6
P15	0.3	0.6	0.3	0.6	0	0	2.7	1.5

Cell Tissue Res. Author manuscript; available in PMC 2011 January 19.